Coding-Based Data Compression for Multichannel SAR

Michele Martone, *Member, IEEE*, Nicola Gollin, Gerhard Krieger, *Fellow, IEEE*, Ernesto Imbembo, and Paola Rizzoli, *Member, IEEE*

***Abstract*— Multichannel synthetic aperture radar (MC-SAR) allows for high-resolution imaging of a wide swath (HRWS), at the cost of acquiring and downlinking a significantly larger amount of data, compared with conventional SAR systems. In this letter, we discuss the potential of efficient data volume reduction (DVR) for MC-SAR. Specifically, we focus on methods based on transform coding (TC) and linear predictive coding (LPC), which exploit the redundancy introduced in the raw data by the finer azimuth sampling peculiar to the MC system. The proposed approaches, in combination with a variable-bit quantization, allow for the optimization of the resulting performance and data rate. We consider three exemplary yet realistic MC-SAR systems, and we conduct simulations and analyses on synthetic SAR data considering different radar backscatter distributions, which demonstrate the effectiveness of the proposed methods.**

***Index Terms*— Data volume reduction (DVR), multichannel (MC) synthetic aperture radar (SAR), raw data quantization, SAR.**

I. Introduction

SYNTHETIC aperture radar (SAR) represents nowadays a well-established technique for the weather- and daylight-independent observation and monitoring of the Earth's surface. Conventional, single-channel SAR is constrained by the well-known limitation on the pulse repetition frequency (PRF) for the achievement of a wide swath width and, at the same time, of a fine azimuth resolution. In this scenario, the use of multiple receiving apertures, mutually displaced in the along-track dimension, allows for achieving high-resolution wide-swath imaging by means of coherent combination of the individual received signals and proper suppression of the ambiguous parts of the Doppler spectra [1], [2]. Such a significant improvement of system capabilities comes at the cost of an increased complexity for the design and realization of a multichannel SAR (MC-SAR), with respect to a single-channel system, together with the generation of a considerably larger volume of data, hence leading to demanding requirements on onboard memory and downlink capacity. In this scenario, it becomes clear that an efficient compression of the SAR raw data represents a task of paramount importance for the design and implementation of MC-SAR missions.

Block-adaptive quantization (BAQ) [3] is the most widely used scheme for SAR data compression and, more recently, novel methods, always grounding on the principle of BAQ, have been suggested. These allow for an improved resource and performance optimization, as the FDBAQ proposed in [4] and the PO-BAQ in [5], and can be combined with the implementation of noninteger data rates [6]. Together with the development of novel SAR system architectures, in the last years efficient data volume reduction (DVR) methods have been proposed, such as the compression scheme based on transform coding (in the range spectrum) introduced for the frequency scan mode in [7], as well as the linear predictive coding (LPC)-based approach for single-channel SAR raw data compression in [8] and [9], with the aim of exploiting the significant azimuth oversampling exhibited by such systems. In the context of MC-SAR, it is worth mentioning the data-driven approach based on the principal component decomposition [10], while the method in [11] makes use of the redundancy among the MC azimuth samples by means of a discrete Fourier transform (DFT) in combination with an optimized bitrate allocation.

In this work, we investigate opportunities and challenges for efficient DVR in MC-SAR. This letter is organized as follows. Section II describes the simulations for the MC data analysis, while Section III presents approaches for efficient DVR for MC-SAR systems. The two considered methods ground on the transform coding (TC)-based method as in [11], and on the LPC paradigm as in [8] and [9]. We investigate the TC- and LPC-based methods in the context of three MC-SAR mission scenarios, and we discuss suitable metrics (autocorrelation, Doppler power spectrum) to assess the properties of the SAR raw signal, together with relevant system parameters impacting the potentials for data compression for MC-SAR. The results, in terms of DVR with respect to the state-of-the-art BAQ method, are presented in Section IV. Finally, conclusions and an outlook are provided in Section V.

II. Analysis of Multichannel SAR Data

In this section, we present the MC raw data analysis using simulated and synthetic data from TanDEM-X.

A. Raw Data Simulations

We consider an MC-SAR system equipped with N receiving subapertures separated in the along-track dimension by a

Received 16 September 2024; revised 24 November 2024; accepted 27 November 2024. Date of publication 2 December 2024; date of current version 11 December 2024. This work was supported in part by European Space Agency (ESA/ESTEC) Project "Data volume reduction for multichannel SAR" under Contract 4000140269/22/NL/AS/kk. *(Corresponding author: Michele Martone.)*

Michele Martone, Nicola Gollin, Gerhard Krieger, and Paola Rizzoli are with the Microwaves and Radar Institute, German Aerospace Center (DLR), 82234 Wessling, Germany (e-mail: Michele.Martone@dlr.de).

Ernesto Imbembo is with European Space Agency (ESA), 2201 AZ Noordwijk-Binnen, The Netherlands.

Digital Object Identifier 10.1109/LGRS.2024.3510433

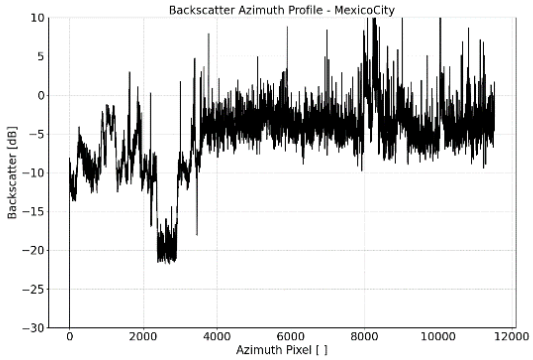

Fig. 1. Backscatter profiles taken from TanDEM-X acquisitions used for the MC-SAR raw data generation taken from the urban area of Mexico City.

distance dx, such that the azimuth antenna length is expressed as $L_a = N \cdot dx$. The sensor flies at velocity v_s and transmits a chirp pulse at $\mathrm{PRF_{Tx}}$. If the uniform sampling condition holds

$$\mathrm{PRF_{Tx}} = \frac{2v_s}{L_a} \tag{1}$$

then the resulting system is equivalent to a single-channel SAR with an effective $\mathrm{PRF_{eff}} = N \cdot \mathrm{PRF_{Tx}}$ and conventional SAR processing can be applied. However, in most cases, due to timing constraints, $\mathrm{PRF_{Tx}}$ must be selected so that (1) is not fulfilled and N (subsampled) channels need to be properly combined to reconstruct the unambiguous Doppler spectrum of the nonuniform azimuth data [1], [2]. As a result, the Doppler bandwidth of the reconstructed MC signal is larger than the transmit $\mathrm{PRF_{Tx}}$, and so a finer azimuth resolution is achieved with respect to a corresponding single-channel SAR operating with the same antenna length L_a and $\mathrm{PRF_{Tx}}$. In this way, MC-SAR is able to image a swath width in the order of 100 km or more with an azimuth resolution down to 1 m [2], [12].

We have generated MC-SAR raw data using a homogeneous backscatter profile, where the power level (variance) of the complex, normally distributed signal is kept constant. In addition, we consider real backscatter profiles from single-look TanDEM-X SAR acquisitions. As an example, Fig. 1 depicts the azimuth profile taken from the area of Mexico City, characterized by urban settlements and rugged topography. In particular, we focus on the azimuth dimension only because of the above-mentioned peculiarities of an MC-SAR, which has high potential for efficient data compression, while in the range dimension the signal properties are in principle similar to the ones of a conventional SAR, hence allowing for limited opportunities for DVR. The azimuth profiles are used to generate, by means of inverse SAR focusing, the N raw data streams, which are then quantized using different compression approaches (i.e., state-of-the-art BAQ as well as TC- and LPC-based schemes). Finally, MC reconstruction, SAR focusing, and performance assessment are carried out.

III. Data Volume Reduction Methods

We now recall and investigate the approaches for DVR to exploit the existing correlation/oversampling among neighboring azimuth samples in MC-SAR: first, we examine the applicability of the Doppler-based TC approach proposed in [11]. Second, we investigate LPC for MC-SAR by applying the method presented in [8] and [9] in the context of single-channel SAR. Preliminary considerations and developments have been presented by Martone et al. [13], while in this letter we provide more detailed discussions and results, also focusing on the relevant descriptors and parameters impacting the achievable DVR.

A. Doppler-Based TC

Following the approach proposed in [11], and referred to as MC-BAQ in the following, the MC-SAR raw data are decomposed by means of a nonadaptive DFT. That is, each MC azimuth raw data block is transformed into the Doppler domain, and then an optimized allocation of the quantization rates is applied to the transformed coefficients, which allows for an increase in the resulting performance for a preselected data rate. For this method, the Doppler power spectrum $P_u(f)$, which describes the signal power distribution among the N azimuth channels, provides information about the achievable coding gain and data compression. In particular, the contribution of the nth channel ${\sigma^2}_n$ is evaluated as [11]

$${\sigma^2}_n \propto P_n \int_{-\mathrm{PBW}/2}^{\mathrm{PBW}/2} \left| \frac{\sin\left(\pi N \frac{f+\mathrm{PRF_{eff}}\cdot(N/2-n)/N}{\mathrm{PRF_{eff}}}\right)}{\sin\left(\pi \frac{f+\mathrm{PRF_{eff}}\cdot(N/2-n)/N}{\mathrm{PRF_{eff}}}\right)} \right|^2 df \tag{2}$$

being f the Doppler frequency. The above equation shows that ${\sigma^2}_n$ is proportional to the square of the Dirichlet kernel of the DFT integrated over the processed bandwidth PBW and scaled by the power associated with the nth transformed coefficient P_n, the latter representing the contribution of the antenna pattern in the corresponding portion of the Doppler spectrum. If the PRF is larger than the processed bandwidth PBW (i.e., the oversampling factor $o_f = \mathrm{PRF_{eff}}/\mathrm{PBW}$ is sufficiently large), then the existing redundancy between subsequent azimuth samples can be suitably exploited by applying the method in [11]. According to this, the achievable DVR is mostly impacted by the following system parameters: antenna pattern shape (and, in turn, L_a, radar wavelength), the number of azimuth channels N, and oversampling factor o_f. Moreover, the target azimuth resolution δa, being related to the PBW, also directly influences the achievable data compression performance.

B. Linear Predictive Coding

We implement the LPC and quantization for DVR in MC-SAR according to the method in [8] and [9] in the context of single-channel SAR. For this purpose, we consider a filter with prediction order $P = [1, 2, 3]$ in the encoding and decoding scheme. Furthermore, we assume that the LPC is restarted for every azimuth block, which means that the first sample is encoded "as is," and then the prediction order P is increased every sample until the target P is reached [9]. In this context, the proposed LPC method can be applied for uniform and nonuniform PRF in the same way.

The achievable coding gain G_P can be derived in closed form based on the autocorrelation values, which describe the spatial coherence and second-order redundancy of a signal and

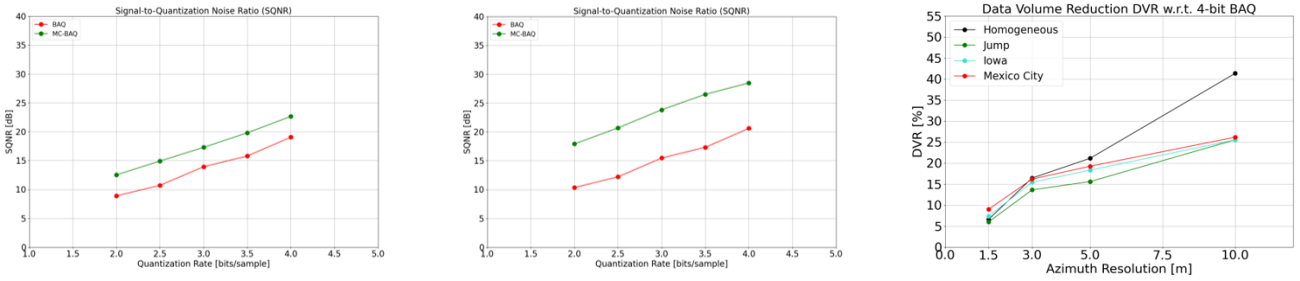

(a) (b) (c)

Fig. 2. SQNR derived for the HRWS C-band system and the homogeneous backscatter profile quantized with a BAQ (in red), and with the method in [11], as a function of the average quantization rate and for (a) $\delta a = 3$ m and (b) $\delta a = 10$ m. (c) DVR (in %) for all simulated profiles and azimuth resolution values.

are related to the specific system [9]. In general, the autocorrelation $R_x(\tau)$ is derived as the inverse Fourier transformation of the raw data power spectral density $P_u(f)$ as a function of the time lag τ. In case of a rectangular antenna aperture, the azimuth autocorrelation is expressed as

$$R_x(\tau) = \mathcal{F}^{-1}\left\{ \sin^4\left(\pi \frac{L_a}{2v_s} f\right) \Big/ \left(\pi \frac{L_a}{2v_s} f\right)^4 \right\} \tag{3}$$

being $\mathcal{F}^{-1}$ the inverse Fourier operator and $B_R = 2v_s/L_a$ the 4-dB bandwidth of $P_u(f)$. One should be aware that (3) assumes that the Tx and Rx patterns are the same: in most cases this does not apply to MC-SAR systems, which typically use the full antenna aperture length together with an appropriate phase spoiling to shape the Tx pattern to optimize the azimuth ambiguity ratio.

For a discrete signal, corresponding to the azimuth SAR raw data signal $x[m]$, $R_x(k)$ can be estimated as a function of the sampled time lag k as

$$R_x(k) = \frac{\sum_{m=0}^{M-1} x[m] \cdot x^*[m+k]}{\sum_{m=0}^{M-1} |x[m]|^2} \tag{4}$$

where M is the number of signal samples and * indicates the complex conjugate. In this work, $R_x(k)$ is estimated assuming a uniformly sampled MC-SAR signal (i.e., the condition in (1) holds), while it is worth highlighting that in general, potential correlation and redundancy in the data can be exploited only within the N-channel azimuth data block. If the MC signal exhibits sufficiently large autocorrelation for small $k > 0$, in addition to LPC, more elaborated schemes such as methods based on the PCA [10] or the JPEG2000 compression standard [14] could be exploited.

By considering the expression in (3), the azimuth autocorrelation (and so the achievable DVR) is determined by the antenna pattern shape (azimuth length, carrier frequency), the number of azimuth channels N, and the PRF. Potential correlation introduced by the statistical properties of the backscatter (i.e., nonfully developed speckle case) may also affect the distribution of $R_x(k)$.

IV. Results and Discussion

In this work, we investigate three MC-SAR system examples, whose relevant parameters are summarized in Table I.

TABLE I
MC-SAR System Parameters

Parameter	ROSE-L-like	HRWS C-band	HRWS X-band
Carrier frequency, f_c	1.25 GHz	5.04 GHz	9.65 GHz
Satellite height, h_s	697 km	697 km	514 km
Antenna type	Planar array		
Acquisition mode	Stripmap		
Azimuth antenna length, L_a	11 m	12.8 m	5.04 m
Number of azimuth channels, N	5	8	[4, 8]
Pulse repetition frequency, $\mathrm{PRF_{Tx}}$ (uniform sampling)	1364 Hz	1188 Hz	3017 Hz
Target azimuth resolution, δ_a	[1.5, 3, 5, 10] m		
Total processed bandwidth, PBW	[4510, 2255, 1353, 676] Hz	[4510, 2255, 1353, 676] Hz	[4691, 2346, 1407, 704] Hz
ADC Resolution	8 bits		

These describe realistic scenarios for future MC-SAR missions at different radar frequencies, such as the ROSE-L [15] or high-resolution imaging of a wide swath (HRWS) systems at the C- and X-band.

The signal-to-quantization noise ratio (SQNR) is used as reference performance metric and is defined as $\mathrm{SQNR} = \sigma_x^2/\sigma_q^2$, where the numerator and denominator represent the power (variance) of the uncompressed signal x and the quantization error q, respectively. The latter is, in turn, defined as $q = x - x_q$, being x_q the quantized signal. The SQNR can be related to SAR and InSAR performance measures, such as the total SNR or the interferometric coherence [5]. For the sake of brevity, performance plots are not shown for all systems but only for selected scenarios, while other cases are commented and summarized in the text. In particular, one should be aware that for the two proposed approaches (TC- and LPC-based), their DVR capabilities are actually influenced by different system parameters: for the TC-based method, the azimuth resolution and the oversampling factor are directly impacting the achievable DVR, while for the LPC-based its performance is principally determined by the autocorrelation of the azimuth raw data, which explains why different parameters and representations were considered for the analysis of the two methods.

The results of the TC-based SAR data compression based as in [11] are summarized in Fig. 2, which shows the SQNR achieved by the proposed method (in green) with respect to a standard BAQ (in red) for the HRWS C-band system. Fig. 2(a) reports the case for $\delta a = 3$ m, resulting in a DVR

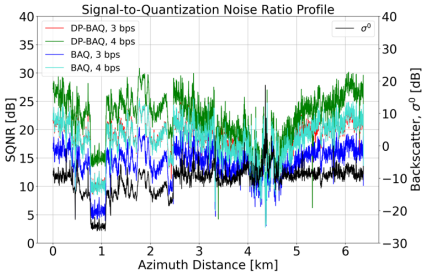

(a)

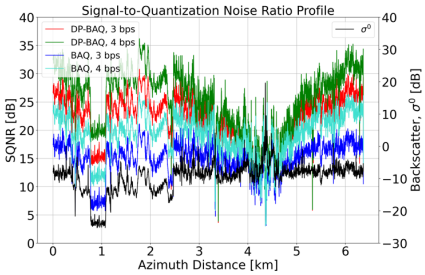

(b)

Fig. 3. SQNR profiles for different quantization schemes (BAQ and first-order DP-BAQ as in [9]) and bitrate (3 and 4 b/s), depicted with different colors, for a backscatter profile over the urban area of Mexico City (shown in black). The X-band HRWS multichannel system is considered for (a) $N = 4$ and (b) $N = 8$ channels.

of about 15%, while Fig. 2(b) shows the significant gain for $\delta a = 10$ m, which is of about 40%. Fig. 2(c) depicts the DVR (in %) for the HRWS at the C-band, for the different simulated profiles as a function of the azimuth resolutions, and a significant increase in DVR can be observed for coarser target azimuth resolutions (i.e., larger oversampling o_f). The different DVR values observed for the 10-m resolution case shows the different impact of the backscatter distribution on the resulting performance degradation—as higher (lower) SQNR is observed for the homogeneous (Mexico City) profile, respectively—for the two quantization schemes (BAQ versus MC-BAQ). For the other two considered systems (L- and X-band in Table I), we obtain a comparable performance, with DVR ranging between 5% and 50% for the fine ($\delta a = 1.5$ m) and coarse ($\delta a = 10$ m) resolution case, respectively.

We now focus on the applicability of LPC for MC-SAR, by implementing the dynamic predictive (DP)-BAQ proposed in [9] in the context of staggered SAR systems. Fig. 3 shows the SQNR for the HRWS X-band system for the case of (a) $N = 4$ and (b) $N = 8$ channels evaluated over the Mexico City profile (in black, right y-axis). The BAQ and the proposed DP-BAQ for 3 and 4 b/s and $P = 1$ are reported with different colors, and a data reduction of about 25% up to more than 50%, for the cases Fig. 3(a) and (b), respectively, is observed.

Table II summarizes the DVR for the considered systems and highlights the potential especially for the X-band HRWS system, where a DVR up to about 50% is achieved, at the cost of a modest additional computational burden (for this analysis, we have considered a prediction order $P = 3$). The large differences in terms of DVR (also considering the negligible values for the C-band HRWS and limited DVR for the ROSE-L-like system) are due to the varying oversampling factors and

TABLE II

DVR (IN % WITH RESPECT TO 4-bit BAQ) USING LPC WITH A PREDICTION ORDER $P = 3$ FOR THE MC-SAR IN TABLE I

	ROSE-L-like	HRWS C-band	HRWS X-band N=4	HRWS X-band N=8
Autocorrelation (k = 1, 2, 3)	0.59, 0.25, 0.18	0.20, 0.18, 0.05	0.89, 0.62, 0.36	0.97, 0.88, 0.75
Homogeneous	7.5%	No reduction	23.3%	42.0%
Iowa	4.7%	No reduction	26.2%	47.2%
Mexico City	1.2%	No reduction	26.1%	54.2%

to the specific azimuth antenna pattern shape, which impacts the resulting autocorrelation values (reported for $k = 1, 2$, and 3 for the homogeneous backscatter profile in the first row of the table). In conclusion, we have demonstrated that the two proposed methods may achieve significantly different performance in terms of DVR depending on the specific system configuration (as an example, the performance of the TC-based method strongly depends on the target azimuth resolution, a parameter which does not influence the performance of the LPC-based method). For this reason, a comparative analysis of the two methods is not straightforward, and each approach needs to be assessed specifically for the system under consideration.

One comment of the anonymous reviewer pointed out the necessity of investigating the impact of the spatial nonuniform sampling and of the amplitude–phase imbalance [16] between the azimuth channels on the achievable DVR. For nonuniform sampling, we have chosen realistic PRF values for the systems under consideration and we have implemented the MC reconstruction according to the method in [1]. Furthermore, we have considered a "light" and a "strong" case for the imbalance, and for this we have assumed deterministic values in the simulation which are kept constant for the whole SAR acquisition. The parameter values used for the present simulations are summarized in Table III. According to these, for the "light" imbalance case, the standard deviation is $\sigma_{G_e} \approx 4\%$ and $\sigma_{\varphi_e} \approx 7.5°$, while for the "strong" imbalance case the standard deviation is $\sigma_{G_e} \approx 15\%$ and $\sigma_{\varphi_e} \approx 36°$, respectively. The impact of nonuniform sampling and amplitude/phase imbalance on the TC-based (MC-BAQ) compression performance is illustrated in Fig. 4 for the HRWS X-band system ($N = 8$ channels, $\delta a = 3$ m, homogeneous backscatter). Here, the SQNR as a function of the quantization rate is shown for different compression schemes and scenarios: with respect to the reference case (i.e., uniform sampling, no imbalance, depicted in green), a worsening of more than 5 dB is observed for the nonuniform and "strong" imbalance case, depicted in pink, leading to a significant loss in terms of the achievable DVR. The performance obtained by BAQ (in red) is not affected by the described effects, while the worsening in performance for the TC-based method is due to the changes introduced by the amplitude and phase imbalances in the resulting Doppler spectrum, such that the (predefined) bitrate allocation does not reflect the actual spectral power distribution [11]. We have carried out the same analysis for the HRWS C-band case ($\delta a = 3$ m, homogeneous backscatter) and consistent results were

TABLE III
PARAMETERS USED FOR ASSESSING THE IMPACT OF NONUNIFORM SAMPLING AND AMPLITUDE/PHASE IMBALANCE

Frequency band	C-band	X-band
Uniform PRF	1172 Hz	3017 Hz
Non-uniform PRF	1265 Hz	3258 Hz
"Light" amp./phase imbalance, G_e, φ_e	G_e =[0.94,0.99,1.06,1.02,0.96,1.05,0.98,1.03] [-] φ_e = [6.1, 2.2, 4.3, -5.4, -7.0, 1.7, 2.3, -4.0] [deg]	
"Strong" amp./phase imbalance, G_e, φ_e	G_e = [1.14,1.21,0.86,1.02,0.76,1.15,0.98,1.13] [-] φ_e = [31.2, -15.0, 14.3, -25.1, -17.5, 11.0, 22.3, -24.2] [deg]	

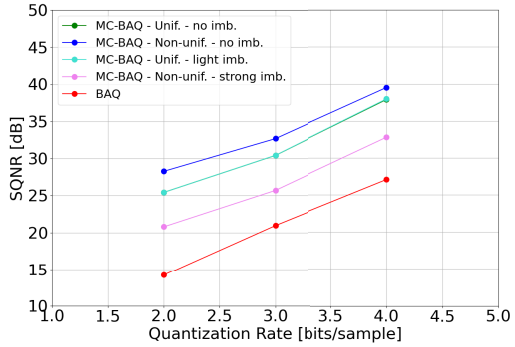

Fig. 4. Impact of nonuniform sampling and amplitude/phase imbalance on the TC-based (MC-BAQ) compression performance for the HRWS X-band multichannel system ($N = 8$, $\delta a = 3$ m) compared with BAQ. SQNR as a function of the bitrate for different sampling and imbalance conditions (reported in Table III), depicted with different colors.

obtained, with the performance of the TC-based compression method (MC-BAQ) being significantly affected in the presence of the "strong" imbalance case only. Finally, we have assessed the described effects on the LPC-based method for the HRWS X-band system ($N = 4$). The results confirm that a significant performance loss is obtained for the "strong" imbalance case and, in particular, the use of high prediction order ($P = 4$) results in a larger degradation, which is due to the less accurate estimation of the azimuth autocorrelation function affecting the filter weights' derivation [9].

V. CONCLUSION AND OUTLOOK

In this letter, we investigated opportunities and limitations for DVR in MC-SAR. We proposed convenient data reduction strategies, aiming at exploiting the existing correlation in the azimuth raw data stream. We introduced relevant parameters to assess the potential for DVR of the MC raw SAR signal and we focused on three system examples. We conducted simulations and suggested suitable approaches for DVR for the MC-SAR systems based on Doppler-based TC [11] and on LPC [8], [9]. We discussed the impact of relevant system parameters and assessed the achievable data reduction with respect to standard BAQ, demonstrating the suitability of the proposed methods for specific MC-SAR configurations. In future studies, we aim at conducting end-to-end performance evaluation on SAR/InSAR performance (i.e., not limited to quantization degradation only), together with an assessment of the nonlinear and signal-dependent impact of SAR compression on different quality measures (e.g., detection, phase), also investigating the potential of the proposed methods for multistatic SAR systems.

ACKNOWLEDGMENT

The authors gratefully acknowledge the valuable suggestions of the anonymous reviewers.

REFERENCES

[1] G. Krieger, N. Gebert, and A. Moreira, "Unambiguous SAR signal reconstruction from nonuniform displaced phase center sampling," *IEEE Geosci. Remote Sens. Lett.*, vol. 1, no. 4, pp. 260–264, Oct. 2004.
[2] N. Gebert, G. Krieger, and A. Moreira, "Digital beamforming for HRWS-SAR imaging: System design, performance and optimization strategies," in *Proc. IEEE Int. Symp. Geosci. Remote Sens.*, Jan. 2006, pp. 1836–1839.
[3] R. Kwok and W. T. K. Johnson, "Block adaptive quantization of Magellan SAR data," *IEEE Trans. Geosci. Remote Sens.*, vol. 27, no. 4, pp. 375–383, Jul. 1989.
[4] E. Attema et al., "Flexible dynamic block adaptive quantization for Sentinel-1 SAR missions," *IEEE Geosci. Remote Sens. Lett.*, vol. 7, no. 4, pp. 766–770, Oct. 2010.
[5] M. Martone, N. Gollin, P. Rizzoli, and G. Krieger, "Performance-optimized quantization for SAR and InSAR applications," *IEEE Trans. Geosci. Remote Sens.*, vol. 60, 2022, Art. no. 5229922.
[6] M. Martone, B. Bräutigam, and G. Krieger, "Azimuth-switched quantization for SAR systems and performance analysis on TanDEM-X data," *IEEE Geosci. Remote Sens. Lett.*, vol. 11, no. 1, pp. 181–185, Jan. 2014.
[7] N. Gollin, R. Scheiber, M. Martone, P. Rizzoli, and G. Krieger, "SAR imaging in frequency scan mode: System optimization and potentials for data volume reduction," *IEEE Trans. Geosci. Remote Sens.*, vol. 61, 2023, Art. no. 5200420.
[8] E. Magli and G. Olmo, "Lossy predictive coding of SAR raw data," *IEEE Trans. Geosci. Remote Sens.*, vol. 41, no. 5, pp. 977–987, May 2003.
[9] M. Martone, N. Gollin, M. Villano, P. Rizzoli, and G. Krieger, "Predictive quantization for data volume reduction in staggered SAR systems," *IEEE Trans. Geosci. Remote Sens.*, vol. 58, no. 8, pp. 5575–5587, Aug. 2020.
[10] P. Guccione, M. Scagliola, and D. Giudici, "Principal components dynamic block quantization for multichannel SAR," in *Proc. IEEE Int. Geosci. Remote Sens. Symp. (IGARSS)*, Jul. 2016, pp. 2090–2093.
[11] M. Martone, M. Villano, M. Younis, and G. Krieger, "Efficient onboard quantization for multichannel SAR systems," *IEEE Geosci. Remote Sens. Lett.*, vol. 16, no. 12, pp. 1859–1863, Dec. 2019.
[12] F. Q. de Almeida, M. Younis, G. Krieger, and A. Moreira, "A new slow PRI variation scheme for multichannel SAR high-resolution wide-swath imaging," in *Proc. IEEE Int. Geosci. Remote Sens. Symp.*, Jul. 2018, pp. 3655–3658.
[13] M. Martone, N. Gollin, E. Imbembo, G. Krieger, and P. Rizzoli, "Data volume reduction for multichannel SAR: Opportunities and challenges," in *Proc. 15th Eur. Conf. Synth. Aperture Radar*, 2024, pp. 1–6.
[14] R. M. Asiyabi et al., "On the use of JPEG2000 for SAR raw data compression," in *Proc. 15th Eur. Conf. Synth. Aperture Radar (EUSAR)*, Munich, Germany, 2024, pp. 249–253.
[15] D. Petrolati et al., "An overview of the Copernicus Rose-L SAR instrument," in *Proc. IEEE Int. Geosci. Remote Sens. Symp.*, Jul. 2023, pp. 4310–4313.
[16] Y. Liu, Z. Li, Z. Wang, and Z. Bao, "On the baseband Doppler centroid estimation for multichannel HRWS SAR imaging," *IEEE Geosci. Remote Sens. Lett.*, vol. 11, no. 12, pp. 2050–2054, Dec. 2014.